

Synthesis of Two Degrees-of-Freedom Haptic Device

Praveen Kumar Singh¹, Subir Kumar Saha^{2*}, and M. Manivannan³

1 Department of Farm Machinery, Mechanical Engineering Research and Development Organization,
Ludhiana-06, India

2 Department of Mechanical Engineering, Indian Institute of Technology Delhi, New Delhi-16, India

3 Department of Applied Mechanics, Indian Institute of Technology Madras, Chennai-36, India

* Email: saha@mech.iitd.ernet.in

Abstract

Haptic devices are force-feedback devices that mediate communication between the user and the computer. Such devices allow users to touch, feel and manipulate three-dimensional objects in virtual environments and tele-operated systems. In this paper, one such device is synthesized for the purpose of training medical students and professionals, specially those requiring force-feedback from the virtual needle inserted into the body. The device is designed to deliver high force. Kinematic analysis of a suitable mechanism is performed and singularities in its workspace were identified to form constraints for an optimization. Performance index based kinematic optimization of the mechanism was performed over the whole workspace. The performance was then checked and limitations were analyzed by means of the so called force manipulability ellipsoid. We found that the performance in terms of kinematic singularity was greatly improved for the optimized mechanism.

Keywords: Haptic devices, Kinematic singularity, Force manipulability ellipsoid, and Performance measure.

1 Introduction

Haptics is the science of touch. It is a recent development in Virtual Environments allowing users to touch, feel, and manipulate the simulated objects with which they interact. Haptic devices can be viewed as having two basic functions: 1) to measure position and their time derivatives accurately, 2) to display contact forces to the user at 1kHz update rate. In this paper, a haptic device is synthesized for virtual epidural injection in which the tip of the needle is inserted into the epidural space within the spinal canal surrounding the spinal cord. The simple haptic device can provide force from an operator to a slave, a slave to an operator, or in both directions, so as to give feedback to the trainee.

Here we synthesize the mechanical part of the device, based on a five-bar planar parallel mechanism. Synthesis of such a manipulator is greatly influenced by the fact that the relationship between the robot's actuators and the end-effector varies with its position and direction. Only after minimizing this variation, or in other words maximizing the mechanical *isotropy*, one can choose suitable actuators and design a controller. The kinematic equations of mechanism describe the relationships between the end-effector and its actuators. The Jacobian matrix then determines the required actuator force/torque from a desired end-effector force/torque.

This paper is organized as follows: Section 2 gives selection criterion; Section 3 presents kinematic modeling, followed by the workspace analysis in section 4. Section 5 presents the kinematic optimization. Finally, accuracy check and conclusions are provided in sections 6 and 7, respectively.

2. Selection Criterion

As of our requirement we desired a device which required two-dimensional positioning, and is accurate in its working workspace, simple, stiffer, and can be easily fabricated. The following are some of the points which were considered before choosing the five-bar parallel architecture shown in Figure 1:

1. Parallel mechanisms are known to provide high stiffness [1], which is required for our application.
2. Errors in individual chains of a parallel manipulator do not directly sum to yield the overall manipulator positioning error [2].

The selected five-bar closed-loop parallel manipulator is simple in its structure, has high stiffness compared to its serial counterpart, and suffers from fewer singularities in its workspace. The device is a grounded planar mechanism which reduces its mass, inertia and frictional force, thereby increasing the sense of realism to the user.

3 Kinematic Modeling

The planar five-bar five revolute jointed parallel mechanism is shown in Figure 1. It has an end-effector point C which is connected to the base by two legs, O₁C and O₂C. In each of the two legs, the revolute joint connected to the base is actuated. The mechanism is symmetric about Y-axis. Such a mechanism can position a point in X-Y plane.

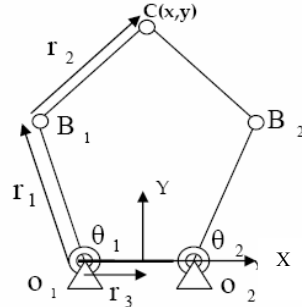


Fig. 1: Kinematic diagram

Let a_1, a_2, a_3 are physical lengths of the mechanism. Then we define normalized lengths as non dimensional parameters $r_i, i=1, 2, 3$, i.e.,

$$r_1 = a_1 / L, \quad r_2 = a_2 / L, \quad r_3 = a_3 / L$$

where, $L = (a_1 + a_2 + a_3) / 3$

3.1 Inverse Kinematics

For inverse kinematics, the location of the end-effector, C is given and the problem is to find the joint variables necessary to bring the end-effector to the desired location [1]. The position vector of the output point C in the reference system X-Y is given by

$$p = (x, y)^T$$

In the reference frame, the position vectors of point B_i (i = 1, 2) can be written as

$$b_1 = (r_1 \cos\theta_1 - r_3, r_1 \sin\theta_1)^T$$

$$\text{and } b_2 = (r_1 \cos\theta_2 + r_3, r_1 \sin\theta_2)^T$$

where, θ_1 and θ_2 are the actuated angles.

The inverse kinematic problem can then be solved by writing the following constraint equations.

$$(x - r_1 \cos\theta_1 + r_3)^2 + (y - r_1 \sin\theta_1)^2 = r_2^2 \quad (1)$$

$$(x - r_1 \cos\theta_2 - r_3)^2 + (y - r_1 \sin\theta_2)^2 = r_2^2 \quad (2)$$

In eqs. (1) and (2), the inputs to reach the position p(x, y) is desired based on the position of point C, obtained. Four solutions are achieved for the inverse kinematic problem.

3.2 Forward Kinematics

The forward kinematics problem is to obtain the output C with respect to a set of given inputs, θ_1 and θ_2 . On solving constrained equations (1) and (2) we get

$$f y^2 + g y + h = 0 \quad (3)$$

in which,

$$f = 1 + d^2, \quad g = 2(d e - d r_1 \cos\theta_1 + d r_3 - r_1 \sin\theta_1)$$

$$h = e^2 - 2e(r_1 \cos\theta_1 - r_3) - 2r_1 r_3 \cos\theta_1 + r_3^2 + r_1^2 - r_2^2$$

From eq. (3), two solutions for the forward kinematic problem are obtained.

3.3 Jacobian Matrix

Let the actuated joint variables be denoted by a vector θ and the location of the moving platform be described by a vector p. Then the kinematic constraints imposed by the limbs can be written in the general form as

$$f(p, \theta) = 0$$

i.e., eqs. (1) and (2)

Differentiating eqs. (1) and (2) with respect to time, we obtain a relationship between the input joint rates and the end-effector output velocity as

$$J_p \dot{p} = J_\theta \dot{\theta} \quad (4)$$

i.e.,

$$J_p = \begin{pmatrix} x - r_1 \cos\theta_1 + r_3 & y - r_1 \sin\theta_1 \\ x - r_1 \cos\theta_2 - r_3 & y - r_1 \sin\theta_2 \end{pmatrix}$$

and

$$J_\theta = \begin{pmatrix} y \cos\theta_1 - (x + r_3) \sin\theta_1 & 0 \\ 0 & y \cos\theta_2 + (r_3 - x) \sin\theta_2 \end{pmatrix} r_1$$

Now, the Jacobian matrix of the five-bar mechanism is given by

$$J = J_\theta^{-1} J_p \quad (5)$$

3.4 Singularity Analysis

Due to the existence of two Jacobian matrices, the mechanism is said to be at a singular configuration when either J_p or J_θ or both are singular. Singularity leads to an instantaneous change of the mechanisms DoF. [1][3]

3.4.1 Inverse Kinematic Singularities

This singularity occurs when the output point reaches its limit or its boundary of the workspace. They are given below:

At,

$$x = (r_1 + r_2) \cos\theta_1 - r_3 \quad \text{and} \quad y = (r_1 + r_2) \sin\theta_1 \quad (6)$$

$$\text{or, } x = (r_1 + r_2) \cos\theta_2 + r_3 \quad \text{and} \quad y = (r_1 + r_2) \sin\theta_2 \quad (7)$$

and

$$x = (r_1 - r_2) \cos\theta_1 - r_3 \quad \text{and} \quad y = (r_1 - r_2) \sin\theta_1 \quad (8)$$

$$\text{or, } x = (r_1 - r_2) \cos\theta_2 + r_3 \quad \text{and} \quad y = (r_1 - r_2) \sin\theta_2 \quad (9)$$

There exists some non-zero $\dot{\theta}$ that results in zero \dot{p} vector. Infinitesimal motion of the end-effector along certain directions cannot be accomplished. Hence manipulator loses one DoF. Under above singularities the links are either fully extended or folded. Hence they are also called

boundary singularities, which are shown in Fig. 2.

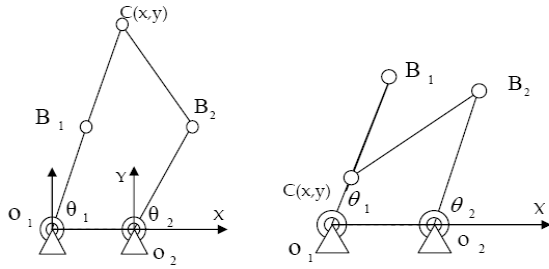


Fig. 2: Boundary singularities

3.4.2 Direct Kinematic Singularities

A direct kinematic singularity occurs when the determinant of J_p is equal to zero.

i.e., $\text{Det}(J_p) = 0$.

The above happens

1) When,

$$r_1 \sin\theta_1 = r_1 \sin\theta_2$$

$$\text{and } r_1 \cos\theta_1 - r_3 = r_1 \cos\theta_2 + r_3$$

i.e. when B_1 and B_2 points coincide.

This singular configuration is shown Fig. 3(a).

2) When,

$$x = (r_1/2) (\cos\theta_1 + \cos\theta_2)$$

$$y = (r_1/2) (\sin\theta_1 + \sin\theta_2)$$

i.e. when point B_1 C B_2 lie on a straight line which is shown in Fig. 3(b).

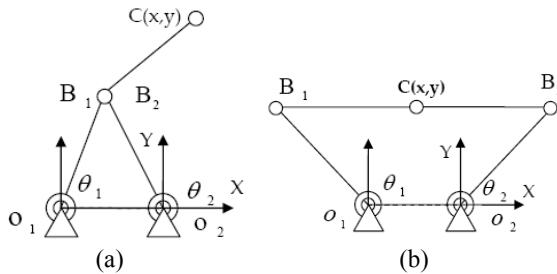


Fig. 3: Direct kinematic singularity

In direct kinematic singularities, there exist some non-zero \dot{p} vectors that result in zero $\dot{\theta}$ vectors. That is, the end-effector can have infinitesimal motion in some directions while all actuators are completely locked. Hence end-effector gains one-DOF.

3.4.3 Conditions for Removing Singularities

In order to avoid the singularities following conditions are obtained.

a) If $r_3 > r_1$, B_1 B_2 will never coincide.

b) If $r_2 > (r_1 + r_3)$

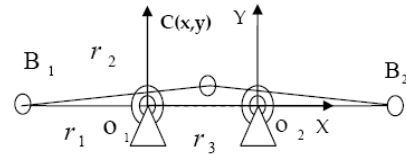


Fig. 4: Combined singularity

B_1 C B_2 will never lie in a straight line.

c) If $r_3 < (r_1 + r_2)$ combined singularity is removed when $O_1 B_1 C B_2 O_2$ will never lie in a straight line.

d) If $r_2 \neq r_3$ combined singularity is also removed, i.e.,

e) $r_1 + r_2 + r_3 = 3$, and $0 < r_1 < 3$, $0 < r_2 < 3$, $r_3 < 1.5$

Rest of the combined singularity conditions are taken care with the above mentioned checks.

4 Workspace Analysis

Workspace of the planar mechanism, Fig. 1 is defined as the space that its end-effector can reach. A dexterous workspace is the space within which every point can be reached by the end-effector from all possible orientations. Boundary singularities describe the boundary of the workspace beyond which the end-effector cannot reach. Equations (6-9) are actually annulus regions within which the workspace lies. As there exist singular loci inside the theoretical workspace the manipulator may pass through them. Hence, there is a need to define a measure of proximity to those singular loci and then accordingly define dexterous workspace.

4.1 Condition Number: Measure of Singularity Proximity and Accuracy

The condition number of the Jacobian matrix can be defined as [1]:

$$C = \sigma_{\max} / \sigma_{\min}$$

where σ_{\max} , and σ_{\min} are the largest and the smallest singular values of the Jacobian matrix, J , respectively. These singular values are equal to the square root of the maximum and minimum eigenvalues of JJ^T where J is the Jacobian matrix. Note that the condition number of a matrix measures the sensitivity of the solution of a system of linear equations to errors in data. It gives an indication of the accuracy of results from matrix inversion and the linear equation solution. Condition number close to one indicates a well conditioned matrix. The condition number is independent of the scale of a manipulator.

To check accuracy we confirm end-effector velocity vector on a unit circle,

$$\dot{p}^T \dot{p} = 1$$

and compare the joint rates as

$$\dot{q}^T J^T J \dot{q} = 1$$

The above equation represents an ellipse in joint space.

The eigen vectors of JJ^T are orthogonal and the principal

axis coincide with them. The lengths of the principal axis are equal to the reciprocals of the square roots of the eigenvalues of JJ^T [4]. Here, the condition number is used for two different purposes: first, as a measure of proximity to singularity; second, as a measure of kinematic accuracy. Using the Inverse kinematics algorithm, position of the end-effector is checked for

1. Solution exists in the joint space or not.
2. The condition number of the Jacobian matrix.

Using the following steps:

- a. Workspace under boundary singularity is divided in a set of circular arcs.
- b. Each point on a circular arc is checked whether solution exists or not in joint space using inverse kinematics.
- c. Then at each point condition number of Jacobian matrix condition number (K) is checked and accordingly given a sign as
 - Plus: if $K < 5$
 - Asterix : if $5 < K < 10$
 - Square: if $10 < K < 100$
 - Diamond: if $K > 100$

From the workspace shown in Fig. 5, we can suggest a region composed of plus sign (with $K < 5$) in which we can work accurately and somewhat singularity free. An annulus region between 0.9 and 1.7 (normalized lengths) can be our dexterous workspace for generalized link lengths taken (which is later optimized) as shown in Fig. 5.

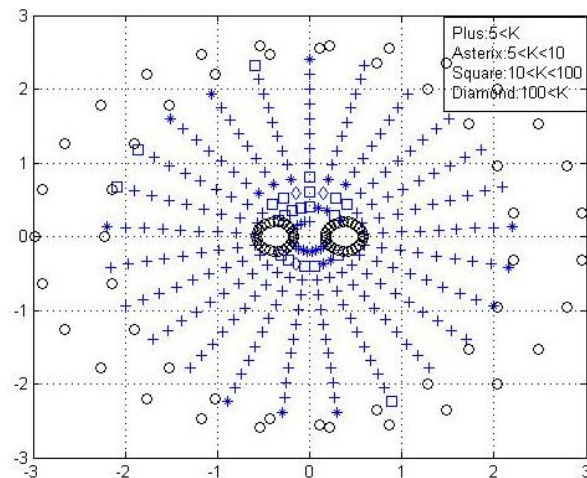


Fig. 5: Plot of Dexterous Workspace

Because the Jacobian is a function of position, the condition number is a local measure and manipulators that are designed to be isotropic at individual positions may not exhibit similar levels of isotropy throughout their workspaces. The condition number only measures the roundness of an ellipse but does not measure its size. Both of these attributes are, however, important in determining the overall consistency of a device's behavior since shape is a relative measurement which represents directional isotropy, which is optimized here.

5 Kinematic Optimization

We see that the condition number of the Jacobian matrix

can be successfully used for performance evaluation and optimization. From the dexterity plot of the workspace with condition number we see that condition number rise high (from 5 to 1000) along the boundaries of manipulator, and we cannot remove the boundary singularities. So, we have to choose performance measure considering the following:

1. Condition number of the Jacobian matrix should rise as smoothly as possible.
2. Condition number should be low at boundaries.
3. Workspace should be more keeping the size of device under certain limit.

Hence, we choose number of workspace points at which condition number is more than 5 as performance measure for optimization.

In this design process, we desire to make the workspace of a device as large as possible and as far away from singularity as possible. We usually select the thickest part in the theoretical workspace as a measure of workspace area. Workspace is characterized by a circle, which is tangent with the singular loci. Here, the circle is referred to as the Maximum Inscribed Circle (MIC), which is defined as the circle that is located at the Y axis and is tangent with the workspace boundary curves. According to this definition, the MIC can be described as

$$x^2 + (y - y_{MIC})^2 = r_{MIC}^2$$

Where,

$$r_{MIC} = \left(\frac{a_1 + a_2 - |a_1 - a_2|}{2} \right)$$

$$y_{MIC} = \sqrt{\left((a_1 + a_2 - |a_1 - a_2|)^2 / 4 - (a_3 / 2)^2 \right)}$$

Some optimization will be performed later with respect to the above r_{MIC} values.

Table 1: Parameter space and optimum

Parameter	Min. value (c.m.)	Max. value (c.m.)	Resolution (c.m.)	Optimum (c.m.)
a_1	9	12	1	10
a_2	11	15	1	15
a_3	3	5	1	3

Design variables are varied as shown in Table 1 and for each architecture, i.e., a combination of a_1 , a_2 and a_3 the "number of points with condition number greater than 5" in the workspace are evaluated. The best configuration is the one for which the "the number of points with $K > 5$ " within the workspace is minimum. The minimum and maximum limits of a_1 , a_2 and a_3 are based on the size of device and other assembling constraints.

Methodology performed for kinematic optimization is give below;

1. Design variables (a_1 , a_2 , a_3) are varied as shown in Table 1.
2. Condition number (K) is found over whole workspace for all possible configurations.
3. Figure 6 is plotted for all architectures for a_3 v/s

- “points with $K>5$ ”.
- From Fig. 6 we select $a_3=3$ due to the minimum of “points with $K>5$ ”.
- In order to find other two link lengths i.e. a_1 and a_2 “Points with $K>5$ ” is checked against the workspace measure (r_{MIC}) for ranges of a_1 and a_2 given in Table 1.

5.1 Results

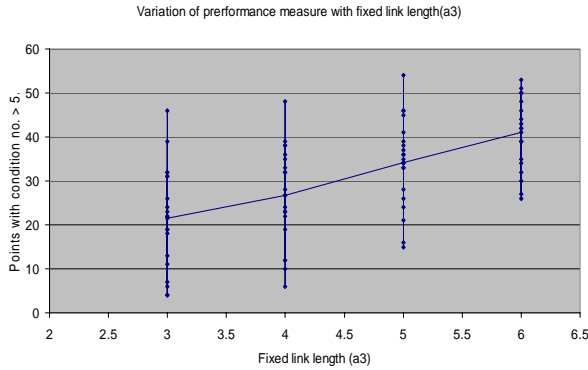


Fig. 6: Variation of performance parameter with base length.

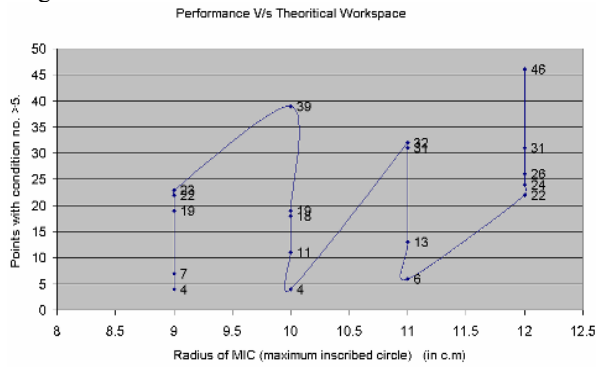


Fig. 7: Graph showing Performance parameter variation with radius of MIC

From Fig. 7 we can see that “Points with $K>5$ ” are minimum corresponding two architectures, i.e. at $a_1=9$; $a_2=14$; $a_3=3$; and $a_1=10$; $a_2=15$; $a_3=3$. Since workspace is higher for latter configuration we chose it as our final design.

6 Accuracy

A force ellipsoid is used for describing the force transmission characteristics of a manipulator at a given posture. Forces in joint space and task space are mapped via Jacobian through the relation.

$$\tau = J^T f \quad (10)$$

Where f is the force vector in task space and τ is the joint torque vector. Using Eq. 13, we obtain

$$f^T f = \tau^T (JJ^T)^{-1} \tau$$

To check the accuracy we confirm the end-effector force vector on a unit circle, i.e.,

$$\|f^T f\| \leq 1$$

It is the ellipse defined by

$$\tau^T (JJ^T)^{-1} \tau \leq 1$$

Similarly for velocity we have,

$$\dot{q}^T J^T J \dot{q} = 1$$

Above equation represents an ellipse in joint space [5].

This ellipse show how efficiently motion/force can be applied in each direction [6]. We see the effect of variation of condition number on force/torque transformation between end-effector and joint space in Fig. 9 which is explained below

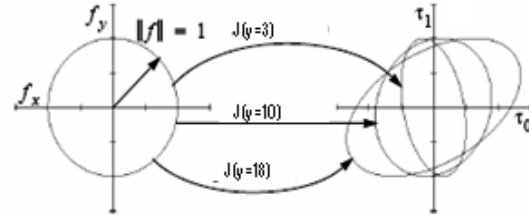


Fig. 8: Force/Torque Transformation

Fig. 8 shows different sizes and shapes of torque ellipses that occur at three different positions of the mechanism analyzed. The ellipses at $y=3$ and $y=18$ have different shapes, i.e., the condition number at $y=3$ are an average of 1.5 times larger than those at $y=18$. In other words it has over one and a half times the average force capabilities in the centre of its workspace than it does at the edges of its workspace.

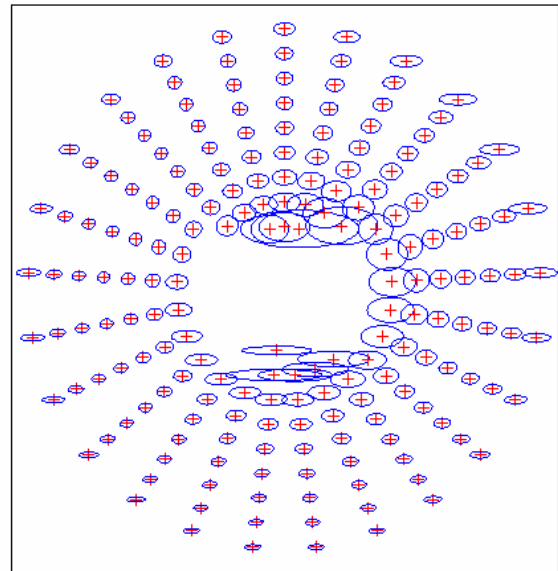


Fig. 9: Graph showing Force/Torque ellipses over the workspace for selected configuration.

Fig. 9 shows the relative sizes of force torque ellipses over the workspace for selected configuration, which is used to check the performance of the proposed design. Fig. 10 shows the photograph of a real prototype made.



Fig. 10: Prototype of synthesized mechanism

ASME Journal of Mechanical Design, 113(3):220-226, 1991.

[7] S. K. Saha, Introduction to Robotics, Tata McGraw-Hill, New Delhi, 2008.

7 Conclusions

A two degrees-of-freedom haptic device is synthesized using a systematic approach. The device has improved performance characteristics which are also analytically analyzed. Based on the above synthesis a prototype of the device was developed, which functioned appropriately. However, further testing is required after interfacing with a virtual environment. This will be taken up in future.

Acknowledgment

This work is supported under IIT Delhi - IIT Madras collaborating project entitled "Development of 2D Haptic Device for Virtual Reality Based Medical Simulation with Haptic Feedback" sponsored by DST, Govt. of India. We take this opportunity to thank all members of Mechatronics Lab, IIT Delhi and Haptics lab, IIT Madras for their supports.

References

- [1] L. Tsai, Robot analysis: The mechanics of serial and parallel manipulators, Wiley & Sons Inc., New York, 1999.
- [2] J. P. Merlet, Parallel Robots. Kluwer Academic Publishers, 2000.
- [3] C. Gosselin, J. Angeles, "Singularity analysis of closed-loop kinematics chains", IEEE Trans. Robotics and Automation, Vol.6, No. 3, pp.281-290, 2006.
- [4] J. O. Kim, P.K. Khosla, "Dexterity Measures for Design and Control of Manipulators", Proc. IROS '91, IEEE/RSJ Int. Workshop Intell. Robots & Sys. (Osaka, Japan), Nov. 3-5, 1991.
- [5] S. Chiu, "Task compatibility of manipulator postures," Int. J. of Robotics Research, 1990.
- [6] C. Gosselin, J. Angeles, "Global performance index for the kinematic optimization of robotic manipulators",